Side-Chain Liquid-Crystalline Homopolymers and Copolymers. Structure and Rheology

A. Wewerka,[†,‡] G. Floudas,[*,†] T. Pakula,[§] and F. Stelzer[‡]

Foundation for Research and Technology-Hellas (FO.R.T.H.), I.E.S.L., P.O. Box 1527, 711 10 Heraklion Crete, Greece, and Physics Department, University of Ioannina, 45 110 Ioannina, Greece; T.U. Graz, Institute of Chemical Technology of Organic Substances (ICTOS), 8010 Graz, Austria; and Max-Planck Institut für Polymerforschung, Postfach 3148, D-55021 Mainz, Germany

Received May 31, 2001

ABSTRACT: We report on the structure and the viscoelastic properties of two side-chain liquid-crystalline polymers with different spacer length in the melt and fiber states and of their copolymers with a semicrystalline block. Optical microscopy, X-ray scattering, and differential scanning calorimetry are employed for the structure investigation and rheology for the dynamics. The smectic and nematic liquid-crystalline polymers exhibit non-Newtonian low-frequency response and violate the empirical principle of time−temperature superposition with the effect being more pronounced in the former. Fibers drawn from the melt exhibit significantly different structure from the melt samples. In the diblock copolymer composed of smectic/crystalline blocks, the strong first-order isotropic-to-smectic transition induces the weak disorder-to-lamellar transition between the dissimilar blocks in the diblock.

1. Introduction

Liquid crystals generally have a rodlike molecular structure and strong dipoles with easily polarizable substituents with a tendecy of the molecules (mesogens) to point along a common axis (director). The high anisotropy of the mesogenic units gives rise to polymorphism, i.e., to the formation of a number of thermodynamically stable phases between the crystalline and isotropic states.[1] Thus, depending on the amound of order in the material, different phases are formed (nematic, smectic, etc.). Polymer liquid crystals (PLC) combine the properties of polymers with those of liquid crystals. These "hybrids" show the same mesophases characteristic of ordinary liquid crystals, yet retain many of the versatile properties of polymers. Main- and side-chain PLC (MC-PLC and SC-PLC) are formed when mesogens are part of the main and side chain, respectively. Another factor influencing the mesomorphic behavior of MC-PLC is the presence of flexible spacers which can decouple the mesogens, thus providing the necessary independent movement of molecules which facilitates proper alignment. However, MC-PLC often cannot show mesogenic behavior over a wide temperature range; SC-PLC, on the other hand, are able to expand this scale.

In the past 20 years, there has been a major interest in the synthesis of such SC-PLC and in understanding the principles of structure formation and structure manipulation by applying external fields.[2−4] The result was new materials with possible commercial applications ranging from high-strength materials for use in optical devices to optically nonlinear devices including optical waveguides and electrooptic modulators in poled polymeric slab waveguides.

A key to many of these applications is their viscoelastic properties in relation to the structure. Earlier studies on SC-PLC melt rheology[5−9] have shown that these materials exhibit unique mechanical properties; for example, unaligned smectics were found to behave as weak viscoelastic solids with nonlinear response at low strains.[8] Furthermore, they exhibit a non-Newtonian behavior which has been attributed to the layered structure that can resist deformation even at very low frequencies.[7−9] In addition, undulations in the layers, defects, and fluctuations can also contribute to the low-frequency behavior. For example, the value of the linear viscoelastic modulus, G_0, obtained at low shear rates/frequencies can only be compared with the k_BT/L^3, if L is chosen to be much larger than the smectic layer spacing d.[8] The expectation is that these length scales are related to the defect texture, and the lower moduli found in the nematic phase would suggest a longer defect spacing. Shear affects the defect texture of such materials; large-amplitude oscillatory shear induces a preferred alignment in SC-PLC.[9]

Block copolymers with one block being a liquid-crystalline polymer have also been synthesized and show different levels of organization;[10−13] the dissimilar blocks favor the microphase separation while the nematic director of the mesogens in the liquid-crystalline block favor the spontaneous orientation in a LC phase. Recently, we reported on the dynamics of two side-chain liquid derivates of poly(norbornene diethyl ester)[14] and their copolymers with the semicrystalline block polyoctene[15] by dielectric spectroscopy. Multiple processes were found in both the homopolymer and the copolymers originating from the backbone and mesogenic units. Quantitatively different dynamics were found in the copolymer with the shorter and longer spacers. The dynamics in the copolymer with the longer spacing were reminiscent of the corresponding homopolymer; however, in the copolymers with the shorter spacer, there was evidence for dynamic mixing between the dissimilar blocks.

Herein we report on the structure and linear viscoelastic properties of two SC-PLC with different spacer lengths in the melt and fiber states and in their

† FO.R.T.H. and University of Ioannina.
‡ ICTOS.
§ Max-Planck Institut für Polymerforschung.
* Author for correspondence. E-mail gfloudas@cc.uoi.gr.

10.1021/ma010944o CCC: $20.00
Published on Web 10/13/2001

copolymers with the semicrystalline block polyoctene. We found that rheology is very sensitive to the smectic-to-isotropic transition and that the strong fluctuations in the smectic and the weaker fluctuations in the nematic phase influence the low-frequency behavior and result in the breakdown of the empirical time−temperature superposition principle. Furthermore, in the copolymers we provide evidence that the strong smectic-to-isotropic first-order transition can induce a weaker transition of the same kind.

2. Experimental Section

Materials. Liquid-crystalline monomers based on a norbornene dicarboxylic acid were synthesized,[16,14] bearing 4′-cyanobiphenyl groups as mesogenic units, which were coupled to the core unit via alkylene-spacers with three or nine methylene groups. The length of the spacer can influence the liquid-crystalline domain structure (i.e., smectic vs nematic). Diblock copolymers have been synthesized, and the second monomer was an absolute cyclooctene that is commercially available.

Scheme 1. Synthesis of LC-monomers

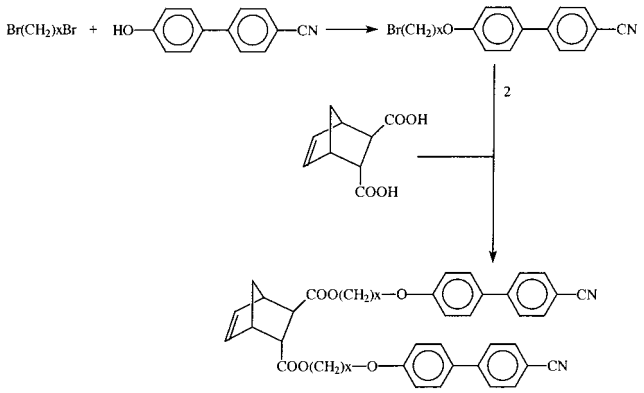

The homo- and the copolymerization reactions were carried out under inert conditions in a glovebox via ROMP (ring-opening metathesis polymerization) employing a Schrock-type molybdenum alkylidene initiator in absolute chlorobenzene. Because of the living character of the ROMP, this methodology provided well-defined polymers with exact molecular weight and low polydispersity. The molecular weights were determined by gel permeation chromatography (GPC) with THF as solvent using the following arrangement: Merck Hitachi L6000 pump, separation columns of Polymer Standards Service, 8 × 300 m STV 5μm grade size (10^6, 10^4, and 500 Å); refractive index detector from Wyatt Technology, model Optilab DSP interferometric refractometer. Polystyrene standards obtained from Polymer Standards Services were used for calibration.

The block copolymerization was carried out by dissolving the monomer A in absolute chlorobenzene and adding the calculated amount of catalyst to start the polymerization of the first block. A sample taken out of this polymerization reaction was studied by ^{1}H NMR until the norbornene double bonds could not be detectable anymore, which provides the time needed for the polymerization of the first monomer. After this particular time, the comonomer B was added to the solution to start the polymerizartion of the second block. The polymers were precipitated from methanol and purified and dried from solvents under vacuum for 2 days.

Optical Microscopy. A Zeiss Axioskop 2 polarizing optical microscope was used together with a Linkam heating stage (THMS 600) and a TP93 temperature programmer (heating and cooling rates of 0.1−90 K/min). The system is also capable of monitoring the kinetics in real time by continuous recording using a CCD camera ($^1/_2$ in. SONY color camera) and a fast frame grabber (capable of up to 50 frames/s) which allows an analysis in terms of the nucleation density, shape, and growth rates using with an appropriate software (Image Pro Plus). The experiments were made by heating to an initial temperature corresponding to the isotropic state followed by subsequent cooling to temperatures corresponding to the liquid-crystalline structures. Subsequently, images were taken while heating the samples over the smectic/isotropic and nematic/isotropic transition temperatures. Representative optical microscopy images for the H9 and H3 homopolymers are shown in Figure 1 with textures exhibiting smectic A and nematic mesophases, respectively. The two images shown for H9 and H3 were taken at 393 and 360 K with the same magnification.

Differential Scanning Calorimetry (DSC). A Polymer Laboratories DSC capable of programmed cyclic temperature runs over the range 113−673 K was used. Samples were first heated with a rate 10 K/min to temperatures corresponding to the isotropic state and subsequently cooled to 153 K with the same rate. The experiment was repeated with several different rates, and the results for the transition temperatures and enthalpies obtained with the lowest rates (4 K/min) are

Scheme 2. ROMP of the homo- and copolymers

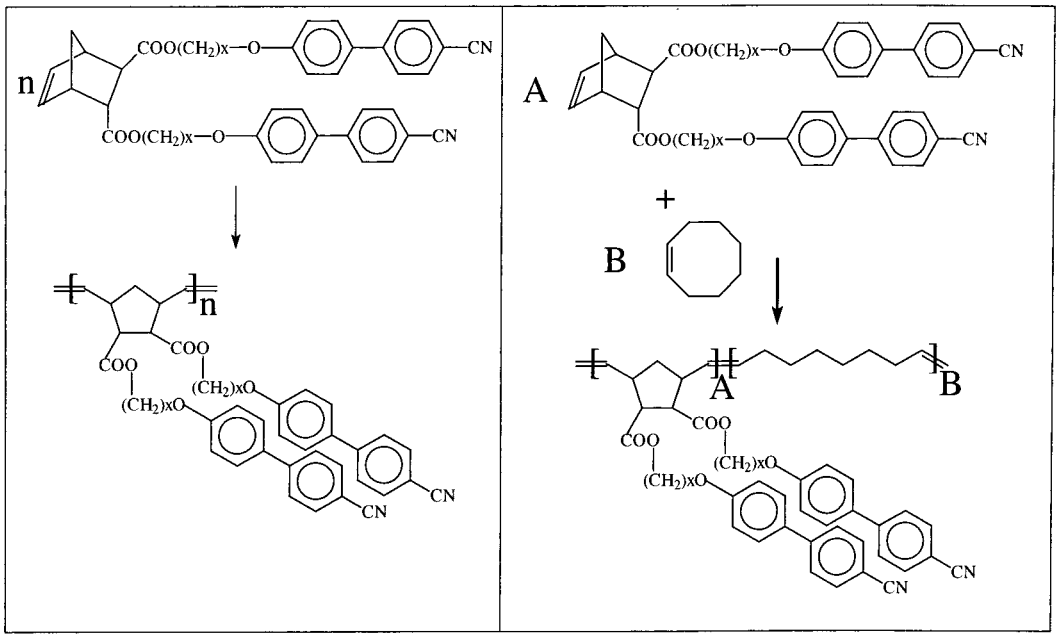

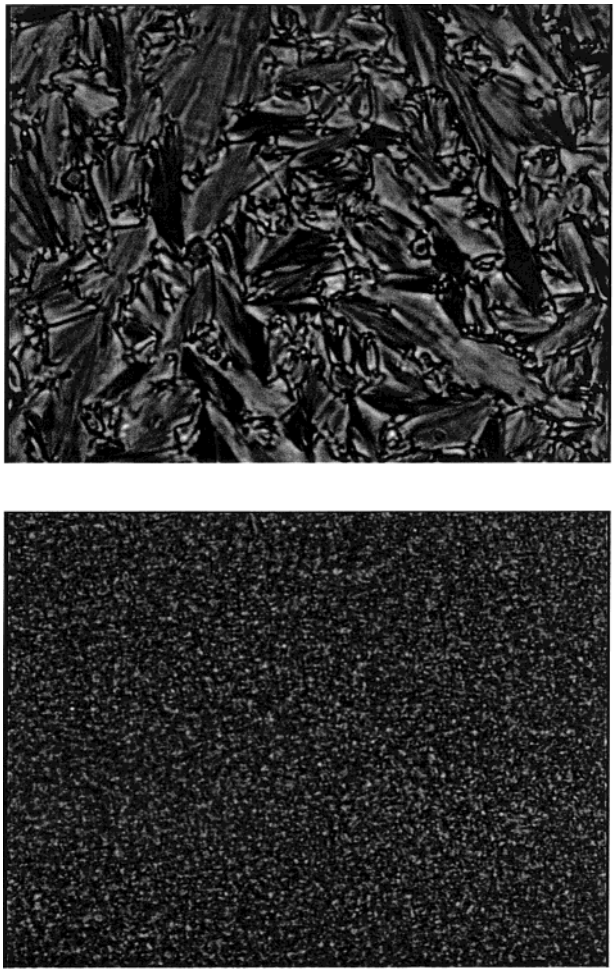

Figure 1. Optical micrographs of the homopolymers H9 (top) and H3 (bottom) thin films observed between crossed polarizers at 393 and 360 K, respectively. The structures can be identified as smectic A (H9) and nematic (H3).

shown in Table 1.

X-ray Scattering. Both WAXS and SAXS measurements have been performed. Two instruments have been employed for the WAXS measurements. For the unoriented samples a Siemens $\theta-\theta$ diffractometer (model D500T) was used in the reflection geometry. The Cu Kα radiation was used from a Siemens generator (Kristalloflex 710 H) operating at 35 kV and 30 mA, and a graphite monochromator was utilized in front of the detector ($\lambda = 0.154$ nm). Measurements were made in the 2θ range from 4° to 60° in steps of 0.01°. We have used the following thermal history: samples were first heated above the melting temperature (to erase any history) and slowly cooled to 203 K. All measurements were made by heating from ambient temperature until the melting temperature. Oriented samples in the form of fibers were studied with an 18 kW rotating anode X-ray source (Rigaku) with a pinhole collimation and a two-dimensional detector (Siemens) with 512 × 512 pixels. The sample-to-detector distance was set to 8.5 cm. All samples were first heated to their isotropic phase in an oven and then slowly cooled to room temperature, allowing for the mesophases to form. Measurements of 2 h long were made at 303 K, with a stability better than ±0.2 K using an appropriate computer program. SAXS measurements were performed with a Kratky compact camera (Anton Paar) equipped with a one-dimensional position-sensitive detector (Braun). The Ni-filtered Cu Kα radiation was used from a Siemens generator. Additional SAXS/WAXS measurements with a higher resolution were made at the X27C beamline of the National Synchrotron Light Source at Brookhaven National Laboratory.

Rheology. An advanced rheometric expansion system (ARES) equipped with a force-rebalanced transducer was used. Both oscillatory shear and steady shear experiments have been performed. In the steady shear experiment the linear and nonlinear viscoelastic ranges have been identified by studying the strain dependence of the amplitude of the complex shear modulus $|G^*|$ $(=(G'^2 + G''^2)^{1/2})$. In the oscillatory shear mode different experiments have been performed: Isochronal temperature scans were made with a frequency of 1 rad/s and a small strain amplitude (the maximum strain amplitude was 2% so that to avoid any shear-induced orientation), aiming to identify the transition temperatures. Subsequently, isothermal frequency sweeps were made at temperatures below and above the transition (obtained by heating), aiming to construct a "master curve". All of these experiments were made with low strain amplitudes, corresponding to the linear viscoelastic regime.

3. Results and Discussion

Homopolymers. Liquid-crystalline phases are normally birefringent and show periodic structures or other textures under crossed polarizers. The interference is due to variations of the optical axis of portions of the phase with respect to the direction of the electric field vector of light. The color in these images is caused by a spatial periodicity of the order of the wavelength of light and interference of the transmitted polarized light. Typical textures include singular points and black threadlike lines (typical of nematic phases) caused by discontinuities in the orientation, mosaic, and fan-shaped textures (typical of smectic phases) and focal conic found in cholesteric and in some smectic liquid crystals. The photomicrographs of the two homopolymers H9 and H3 (Figure 1)—taken from samples slowly cooled from the isotropic phase—show textures that resemble smectic A and nematic phases, respectively. However, the liquid-crystalline order is relatively weak as indicated by the absence of strong reflections in the WAXS spectra of the homopolymers.

Figure 2 compares the thermogram of the H9 homopolymer on cooling and subsequent heating with a rate of 10 K/min with the storage modulus. In accord with the OM study, in DSC, there is an endothermic peak at about 408 K with a heat of fusion of 5 J/g associated with the first-order smectic-to-isotropic transition. The storage modulus obtained under isochronal conditions ($\omega = 1$ rad/s) displays a decrease within the range 390−410 K, which is suggestive of a phase transition. The frequency dependence of the storage and loss moduli, shown in Figure 3a, nicely display the effect of the phase transformation on the viscoelastic properties of this complex material. The $G'(\omega)$ and $G''(\omega)$ spectra, obtained during the isothermal frequency scans, were subsequently shifted to the corresponding spectrum at 373 K. Strictly speaking, the use of time−temperature superposition (tTs) is not valid in systems with a T-dependent order parameter such as liquid crystals[7] and block copolymers.[17,18] Nevertheless, we still show the result of the attempted tTs to illustrate how the different processes affect the viscoelastic response of the system in the vicinity of the transition. Starting from higher frequencies, the spectra for the storage and loss moduli display a power-law dependence as $\omega^{1/2}$, which is frequently found in systems with layered structure such as lamellar-forming block copolymers. This weak frequency dependence extends to the low-frequency side of the spectra taken at higher temperatures. Again, the non-Newtonian behavior is due to the layered structure that can resist deformations

Table 1. Molecular Characteristics and Transition Temperatures of the Homopolymers and Block Copolymers[a]

sample	M_w	PDI	M_z	T_g (K)	T_{trans} (K)	ΔH (J/g)
homopolymer H3	35 200	1.44	48 200	344	$N \xrightarrow{383} I$	~0.6
homopolymer H9	27 000	1.58	45 500	294	$S \xrightarrow{408} I$	5
copolymer C3	85 400	2.88	54 100	348	$C + N \xrightarrow{370} I + O \xrightarrow{403} I + D$	~0.3[b]
copolymer C9	34 400	1.44	48 600	294	$C + S \xrightarrow{330} S + O \xrightarrow{408} I + D$	13, 5.4

[a] I = isotropic; N = nematic, S = smectic, C = semicrystalline, O = ordered, D = disordered. [b] Refers to the nematic-to-isotropic transition.

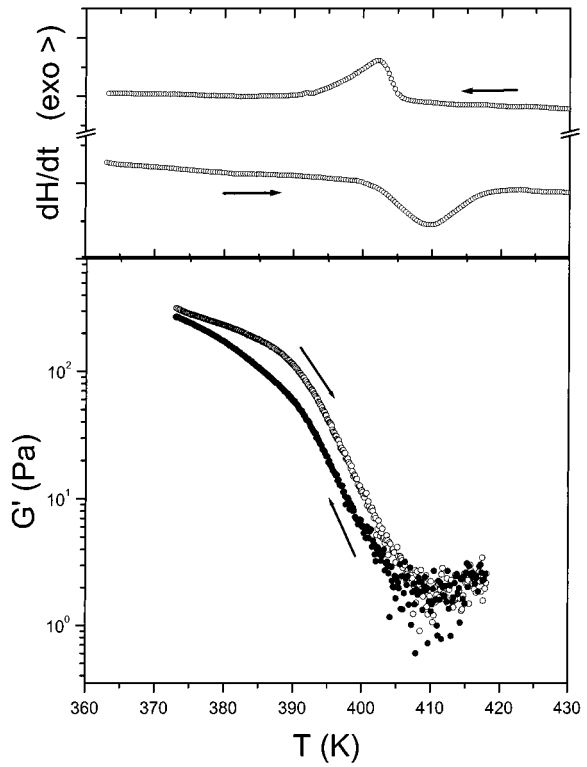

Figure 2. Heat flow (top) and storage modulus (bottom) of H9 obtained during heating and subsequent cooling in DSC and rheology. In DSC the heating and cooling rate was 10 K/min whereas in rheology 2 K/min. Notice that the first-order transition associated with the smectic-to-isotropic transition is also reflected by the drop of the storage modulus within the same temperature range. The storage modulus was measured with $\omega = 1$ rad/s with a strain of 1%.

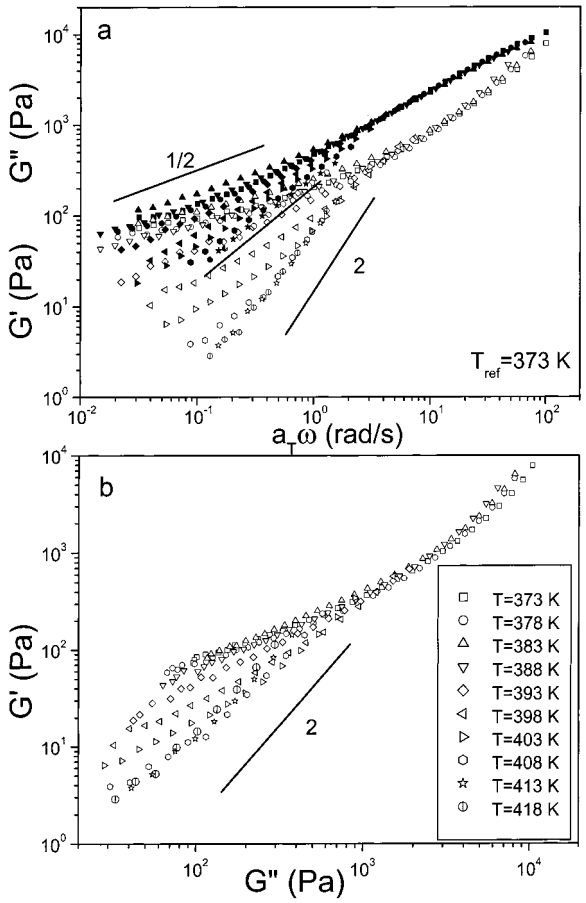

Figure 3. (a) Attempted "master curve" construction for the storage (open symbols) and loss (filled symbols) moduli through the use of tTs for the H9. The reference temperature was 373 K. A single frequency scale shift factor a_T allows superposition only of the high-frequency part of the spectra taken at different temperatures to the spectrum at the reference temperature. Lines with slopes $^1/_2$, 1, and 2 are shown and compared with the low-frequency behavior in the smectic and isotropic states. (b) G' vs G'' representation (known as the Han representation) of the unshifted data. All data were taken by heating with low deformations corresponding to the linear viscoelastic regime.

at low frequencies because of very long terminal relaxation times. At 408 K, the viscoleastic response of the system becomes fluidlike with low-frequency slopes approaching the Newtonian behavior (1 and 2 for the loss and storage moduli, respectively) characteristic for the terminal flow range. Notice, however, that even at the highest temperature investigated (418 K), which is located some 10 K above the transition ($T_{SI} = 408$ K), the storage modulus at low frequencies displays a somewhat lower slope than the one expected for a true Newtonian response in the terminal zone.

Another way of determining the transition temperature—which does not require the use of tTs—is by plotting the logarithm of the storage moduli as a function of the logarithm of the loss moduli for the different temperatures (known as the Han representation[19]). In this representation, the homogeneous phase corresponds to a temperature where the slope attains a value of 2. The result of this representation is shown in Figure 3b for the H9. According to this Figure, the first T where the slope attains a value of 2 is at 408 K; therefore, the two representations give identical results for the transition temperature ($T_{SI} \approx 408$ K). Notice that the deviation from a slope of 2 at the lowest frequencies persists. The deviation from the Newtonian response at temperatures above the transition may reflect on some local order above the transition originating either from (i) pretransitional effects and/or (ii) a narrow, albeit weak, nematic phase.

The corresponding results for the nematic liquid-crystalline polymer H3 are shown in Figures 4 and 5. The thermogram shown in Figure 4, obtained on cooling and subsequent heating, displays a step at about 344 K, signifying a glass transition and a weak endothermic peak at about 373 K with a latent heat of 0.6 J/g. The lower latent heat can be identified with the nematic-to-isotropic transition and reflects the lower order in the material as opposed to smectic phases. The storage

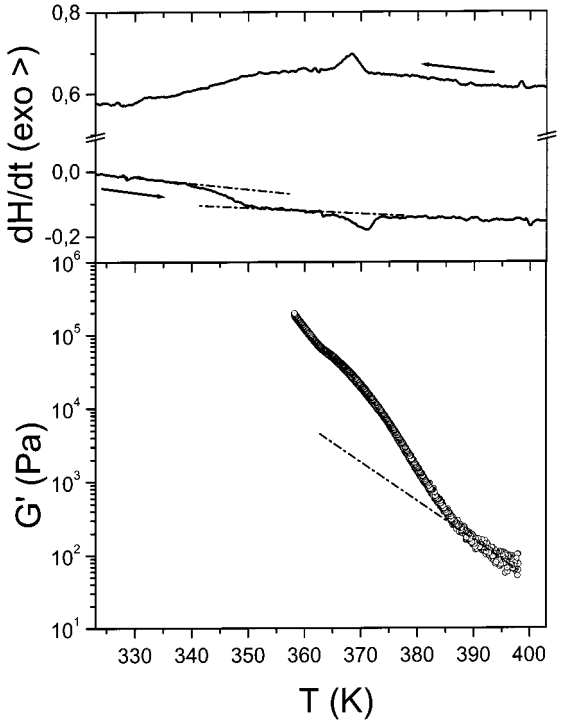

Figure 4. Heat flow (top) and storage modulus (bottom) of H3 obtained during heating and subsequent cooling in DSC and rheology. In DSC the heating and cooling rate was 10 K/min whereas in rheology 2 K/min. Notice the first-order transition associated with the nematic-to-isotropic transition in DSC and the concomitant decrease of the storage modulus within a broader temperature range.

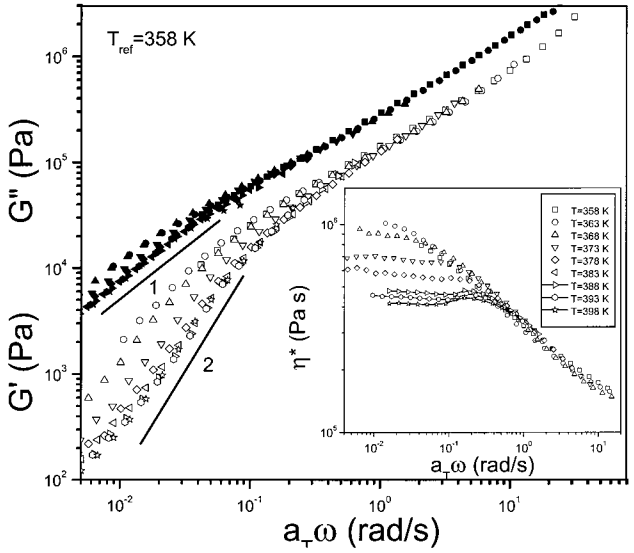

Figure 5. Attempted "master curve" construction for the storage (open symbols) and loss (filled symbols) moduli through the use of tTs for the H3. The reference temperature was 358 K. A single frequency scale shift factor a_T allows superposition only of the high-frequency part of the spectra taken at different temperatures to the spectrum at the reference temperature. Lines with slopes 1 and 2 are shown. In the inset the shifted viscosity spectra are also shown.

modulus, shown also in Figure 4, displays a decrease over a broader temperature range.

The result of the attempted tTs is shown in Figure 5 and reveals qualitatively similar behavior with the H9. As with the H9 homopolymer, tTs does not work, especially at temperatures below 383 K and at low frequencies. On the basis of the result from the shifted

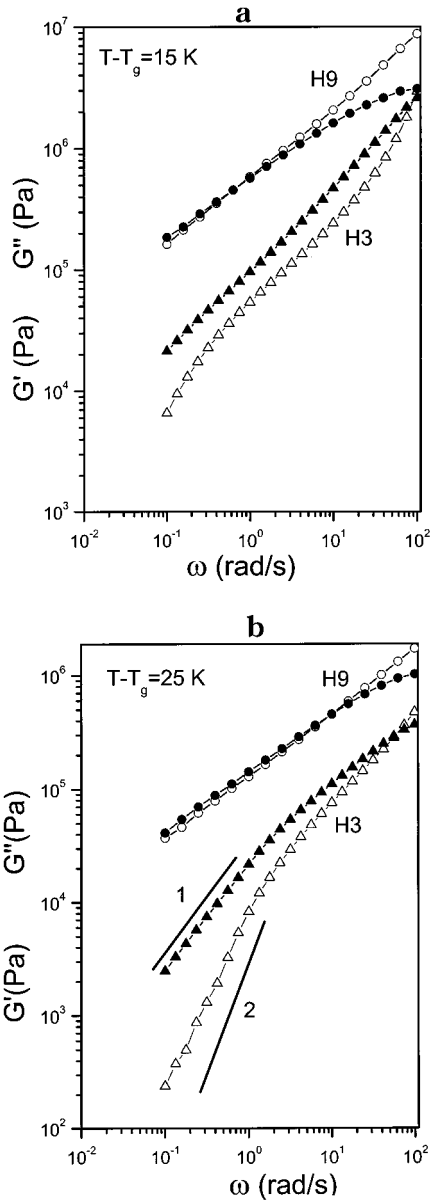

Figure 6. Comparison of the viscoelastic spectra of the H9 and H3 in their smectic and nematic phases at temperatures equidistant from the individual glass transition. Top: comparison at $T - T_g = 15$ K (actual temperatures are 313 and 363 K for H9 and H3, respectively. Bottom: comparison at $T - T_g = 25$ K (actual temperatures are 323 and 373 K for the H9 and He, respectively).

spectra, we assign the nematic-to-isotropic transition at 383 K. There is, however, a difference from the H9; the effect of fluctuations is smaller on the low-frequency moduli, and the loss moduli display low-frequency slopes very near to the slopes expected at the terminal relaxation, however, without obeying the tTs. This implies that the low-frequency response below the transition in H3 is dictated by weak fluctuations and a low number of defects.

The viscoelastic properties of the smectic and nematic liquid-crystalline polymers can best be discussed by comparing spectra taken at temperatures equidistant from the corresponding glass transitions (T_g(H3) = 344 K, T_g(H9) = 294 K). This comparison is made in Figure 6 at temperatures 15 and 25 K above the individual glass transitions. At these temperatures both homopolymers are in their liquid-crystalline mesophases. The

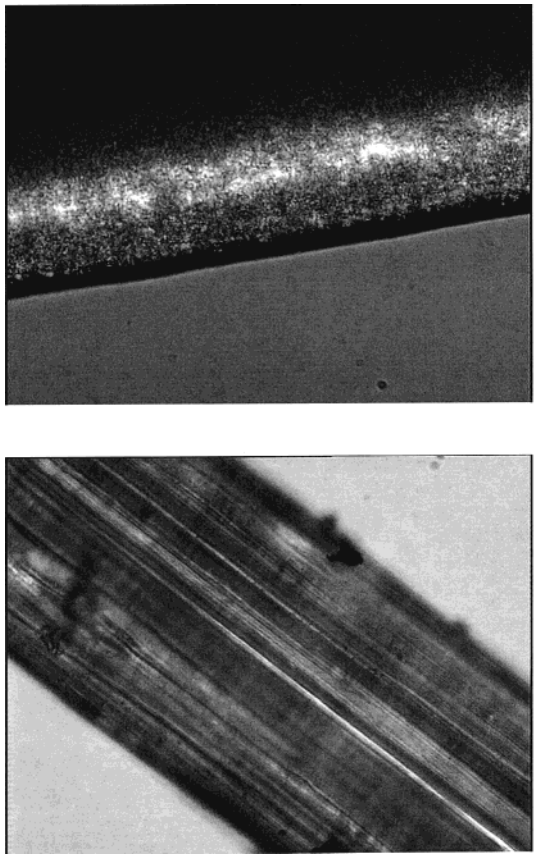

Figure 7. Optical micrographs of H9 (top) and H3 (bottom) fibers taken at 373 and 353 K, respectively.

response of H9 in the smectic phase is viscoelastic ($G'(\omega) \approx G''(\omega)$) over the whole frequency range. In contrast, the nematic phase of H3 shows liquidlike response ($G'(\omega) > G''(\omega)$) without displaying the true Newtonian behavior at low frequencies (i.e., the $G'(\omega)$ slope is lower than 2).

Homopolymer Fibers. Fibers could be pulled directly from the melt for both homopolymers. Samples were heated on a hot plate, and the tip of a glass was used to draw fibers which were formed under rapid cooling and high deformation.[20] The optical micrographs from such fibers are shown in Figure 7 and display qualitatively different order than the homopolymer melts: the H9 fiber indicates a nematic-like order whereas the H3 fiber displays a smectic-like order. To examine the morphology of the samples in their fiber state, we have studied their diffraction patterns at room temperature. Figure 8 gives the scattering patterns for the H9 and H3 fibers. A first inspection shows that qualitatively different structures are obtained. The pattern of H9 exhibits broad meridional reflections at wide angle with a corresponding distance of 0.44 nm and equatorial peaks at smaller angles corresponding to a distance of 2.09 nm. The pattern of H3 shows only broad equatorial reflections at wide angles with a corresponding distance of 0.44 nm. The similar spacings obtained from the wide-angle diffraction may suggest intramolecular correlations within the liquid-crystalline side group. In the H9 fibers, the wide-angle peak being in the same direction as the draw direction can suggest a model as in the schematic shown in Figure 9 (top) where the backbones are oriented along the fiber axis and the liquid-crystalline groups are oriented parallel to the backbone. In the H3 fibers, the wide-angle peak being in a direction perpendicular to the draw direction can suggest the model shown in Figure 9 (bottom), where the backbones are oriented along the fiber axis but at a higher separation than in H9 and the liquid-crystalline groups are oriented perpendicular to the draw direction.

The diffraction patterns of the fibers demonstrate the existence of a nematic- and smectic-like order in the H9 and H3 homopolymers, respectively. We have to keep in mind, however, that the diffraction patterns shown Figure 8 were obtained following high deformation and fast cooling from high temperatures; thus, the suggested structures are those obtained by the polymers following a fast relaxation from the isotropic state.

Copolymers. The two copolymers synthesized, composed of a liquid-crystalline block and the semicrystalline block polyoctene, offer the possibility of studying the structure and the corresponding dynamics in the semicrystalline, the liquid-crystalline, and the block copolymer ordered and disordered as well as in the isotropic states. The structure was first investigated by OM, which indicated the respective formation of a smectic and a nematic phase in the copolymers C9 and C3. However, the textures observed were limited to smaller scales than in the H9 homopolymer. To establish the structure on the relevant length scales, we performed WAXS aiming to follow the crystallization/melting of the semicrystalline block. The diffraction spectra show that the melting of the crystallizable block in the copolymer occurs at about 330 K, in agreement with the pure cyclooctene. The DSC thermogram obtained on heating with a rate of 10 K/min shown in Figure 10 revealed two endothermic peaks at 330 and 402 K with corresponding heats of fusion of 13 and 5.5 J/g. The first and more intense reflects the melting of the semicrystalline block (the heat of fusion of the pure polyoctene is 25 J/g) and scales with block composition. The higher one occurs at exactly the same temperature as the smectic-to-isotropic transition of the homopolymer H9; however, the heat of fusion associated with the transition in C9 is even higher than the H9 despite the smaller fraction of the H9 block in the copolymer. The excess heat content in C9 results from the simultaneous smectic-to-isotropic and order-to-disorder transitions at 408 K. That is, by decreasing temperature from the high-T isotropic phase, the following phases appear: the strong first-order transition associated with the isotropic-to-smectic transition induces the microphase separation of the unlike blocks at the same temperature. This creates an interesting situation of two coupled first-order transitions. At lower temperature, the microphase-separated system is composed from an amorphous polyoctene block and a layered smectic block. At about 330 K, crystallization of the polyoctene block starts, and the system is composed from a semicrystalline block and a smectic block. At 294 K, the mobility within the smectic phase freezes at the smectic-to-glass transition.

The above transitions are nicely reflected in the viscoelastic response of the system at the different temperatures. In Figure 10, the storage modulus of C9 displays discontinuous decreases at 330 and 408 K, which correspond to the two endothermic peaks in DSC (Figure 10, top). To investigate further the viscoelastic response in the different states, we performed frequency sweeps and shifted the G' and G'' spectra to the corresponding spectra at a reference temperature (T_{ref} = 343 K). The result of the attempted tTs is shown in

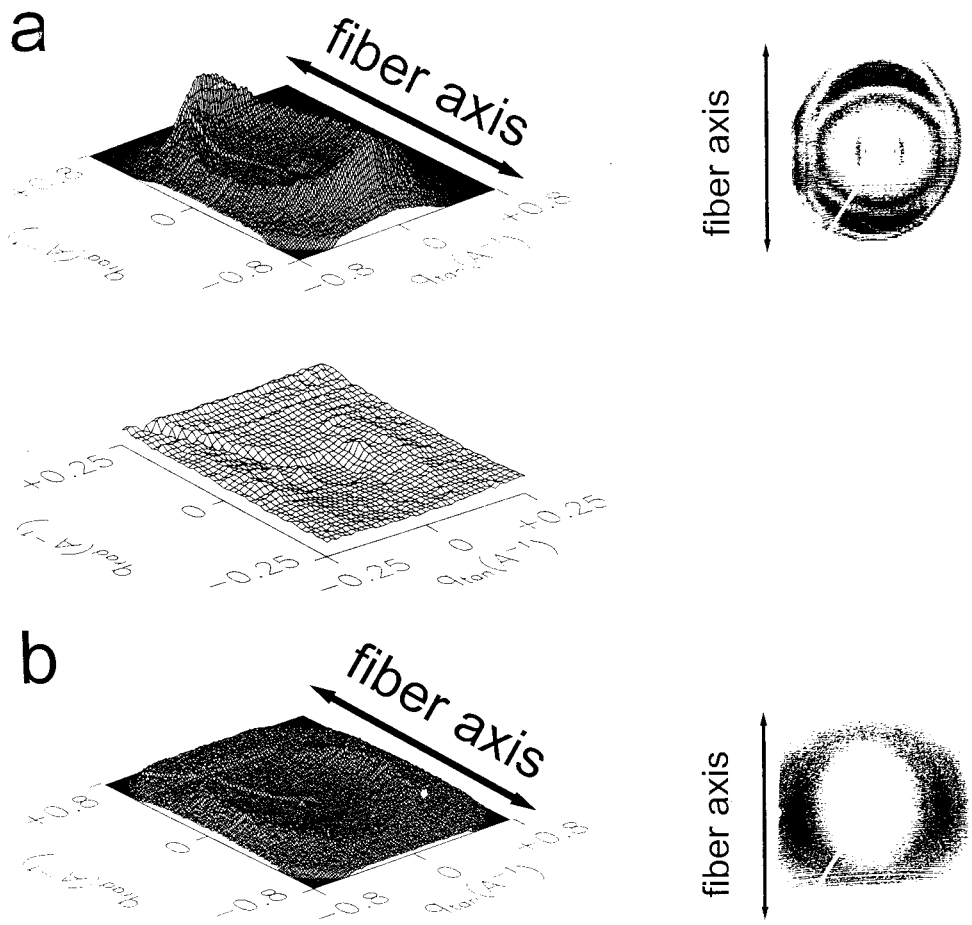

Figure 8. 2-D WAXS patterns obtained at room temperature from (a) H9 and (b) H3 fibers. The second 2-D pattern for H9 depicts the anisotropy near the center of the top pattern. Notice that in H9 the wide-angle peak is in the same direction as the draw direction whereas in H3 the wide-angle peak is perpendicular to the draw direction. Moreover, equatorial peaks exist in the H9 with orientation perpendicular to the draw direction.

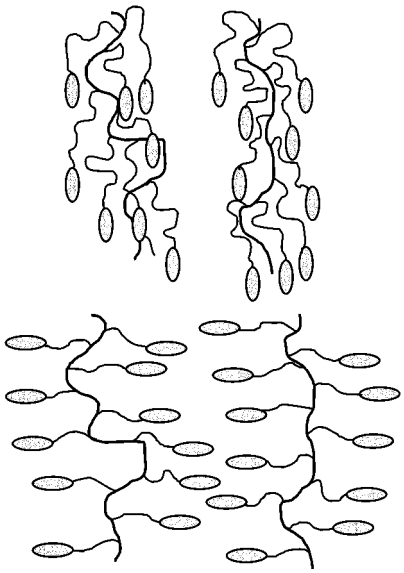

Figure 9. Schematic representation of the local structure in the H9 (top) and H3 (bottom) fibers.

Figure 11. In the same figure the result of the G' vs G'' representation is shown. As with the H9, the tTs fails to describe the viscoelastic response over a broader frequency range, but this now results from two kinds of order: the liquid-crystalline and the block copolymer order. Again, both representations result in the same transition temperature (408 K) which is identical with the smectic-to-isotropic transition in the H9. The low-frequency viscoelastic moduli of ordered block copolymers exhibit a power-law dependence below the order-to-disorder transition and a Newtonian flow behavior above the ODT. In the present case, the T_{ODT} of the diblock copolymer coincides with the T_{SI} of the liquid-crystalline block; that is, the strong first-order transition associated with the smectic-to-isotropic transition induces the weaker first-order transition associated with the order-to-disorder transformation.

Subsequently, the structure in the C9 copolymer was investigated. To enhance the orientational order, fibers pulled from the melt were investigated by WAXS. Wide-angle and smaller-angle peaks with positions similar to the homopolymer H9 (corresponding distances of 0.45 and 2.2 nm) have been obtained. Efforts to measure the period of the block copolymer lamellae (using synchrotron SAXS at BNL, beamline X27) failed due to the low contrast or the very long distances involved.

The phase behavior of the C3 copolymer is very different. In DSC, only one endothermic peak was found at 370 K (heat content 0.3 J/g), without a clear crystallization/melting of the semicrystalline block. The suppressed crystallization as well as the shift of the nematic-to-isotropic transition indicates some mixing between the two blocks. This picture is in agreement with the dielectric spectroscopy study[15] which has shown dynamic mixing between the dissimilar blocks in C3. Furthermore, the high-temperature phase is still ordered as was indicated by the viscoelastic properties

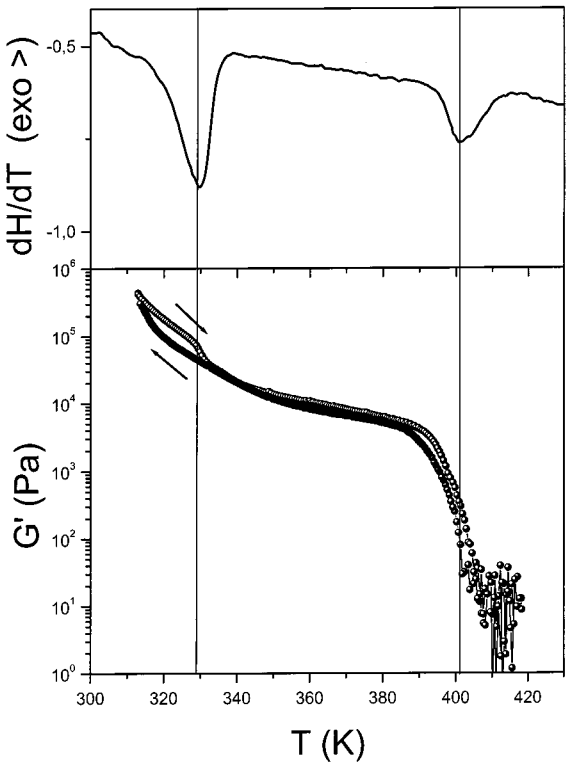

Figure 10. Heat flow (top) and storage modulus (bottom) of C9 obtained during heating in DSC and rheology, respectively. In DSC the heating and cooling rate was 10 K/min whereas in rheology 2 K/min. Notice the two first-order transitions associated with the melting of the semicrystalline block (at 330 K) and the smectic-to-isotropic transition (at 408 K) which are reflected by the endothermic processes and by the drop of the storage modulus within the same temperature range. The storage modulus was measured with $\omega = 1$ rad/s with a strain of 1%.

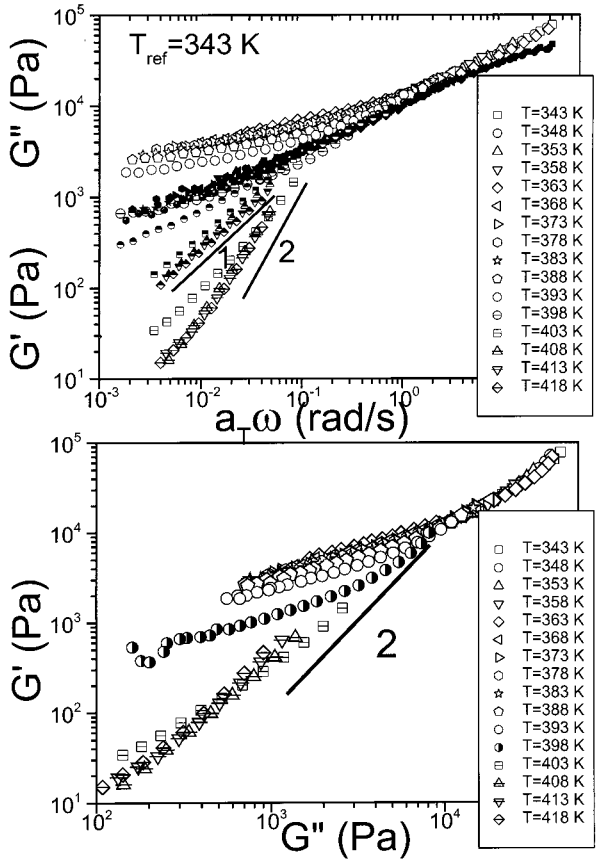

Figure 11. (top) Attempted "master curve" construction for the storage (open symbols) and loss (full and half-filled symbols) moduli through the use of tTs for the C9. The reference temperature was 343 K. Lines with slopes 1 and 2 are shown. (bottom) G' vs G'' representation of the unshifted data which results in an identical transition temperature (T = 408 K). All data were taken by heating with low deformations corresponding to the linear viscoelastic regime.

of the copolymers. Above the nematic-to-isotropic transition and for temperatures up to 403 K, the copolymer remains in the microphase-separated state as evidenced by the weak frequency dependence of the low-frequency moduli.

The results above reveal quantitatively different behavior in the block copolymers with smectic and nematic mesophase structure. The strong first-order transition associated with the isotropic-to-smectic transition within the LC block was found to drive the weaker first-order transition associated with the microphase separation of the dissimilar blocks in the diblock. In contrast, in the nematic forming system, two weak first-order transitions exist which are decoupled.

4. Conclusion

The results of the structure and viscoelasticity on the two SC-PLC and their copolymers with the semicrystalline block polyoctene can be summarized as follows:

1. Both nematic and smectic PLC's show the non-Newtonian low-frequency response for a range of temperatures that results in the failure of the empirical time−temperature superposition principle. The effect is more pronounced in the smectic phase. Apparently, the nematic phase is characterized by weak fluctuations and/or a lower number of defects.

2. Fibers obtained by high deformation and fast cooling have shown the formation of different structures as compared to the melt; i.e., the PLC with the longer spacing, which in the melt forms a smectic phase, in the fiber exhibits nematic-like order.

3. The structure and viscoelastic properties of the two copolymers based on a semicrystalline block (polyoctene) and the smectic and nematic forming blocks have shown quantitatively different behavior: the strong first-order isotropic-to-smectic transition within the LC block was found to drive the weak first order disorder-to-lamellar transition between the dissimilar blocks in the diblock. In contrast, in the nematic SC-PLC, two weak first-order transitions exist (nematic-to-isotropic and order-to-disorder) which are decoupled.

In parallel with the present study we have investigated the local dynamics in the same SC-PLC homopolymers[14] and diblock copolymers[15] with polyoctene by dielectric spectroscopy. We found that the higher order in the smectic-forming SC-PLC reflects on the local dynamics with the appearance of a slow process reflecting the mesogens dynamics within the smectic layers. Moreover, pressure was found to have a stronger influence on the smectic-to-isotropic transition as compared to the glass temperature.

References and Notes

(1) de Gennes, P. G.; Prost, J. *The Physics of Liquid Crystals*; Clarendon Press: Oxford, 1993.
(2) Finkelmann, H.; Rehage, G. *Adv. Polym. Sci.* **1984**, *60*, 90.

(3) Shibaev, V. P.; Plate, N. A. *Adv. Polym. Sci.* **1984**, *60*, 173.
(4) Finkelmann, H.; Ringsdorf, H.; Siol, W.; Wendorff, J. H. *ACS Symp. Ser.* **1978**, *74*, 22.
(5) Pakula, T.; Zentel, R. *Makromol. Chem.* **1991**, *192*, 2401.
(6) Colby, R. H.; Gillmor, J. R.; Galli, G.; Laus, M.; Ober, C. K.; Hall, E. *Liq. Cryst.* **1993**, *13*, 233.
(7) Larson, R. G.; Winey, K. I.; Patel, S. S.; Watanabe, H.; Bruinsma, R. *Rheol. Acta* **1993**, *32*, 245.
(8) Colby, R. H.; Ober, K.; Gillmor, J. R.; Conelly, R. W.; Duong, T.; Galli, G.; Laus, M. *Rheol. Acta* **1977**, *36*, 498.
(9) Kannan, R. M.; Kornfield, J. A.; Schwenk, N.; Boeffel, C. *Macromolecules* **1993**, *26*, 2050.
(10) Fischer, H.; Poser, S. *Acta Polym.* **1996**, *47*, 413.
(11) Sanger, J.; Gronski, W.; Maas, S.; Stuhn, B.; Heck, B. *Macromolecules* **1997**, *30*, 6783.
(12) Anthamatten, M.; Hammond, P. T. *Macromolecules* **1999**, *32*, 8066.
(13) Fingueiredo, P.; Geppert, S.; Brandsch, R.; Bar, G.; Thomann, R.; Spontak, R. J.; Gronski, W.; Samlenski, R.; Muller-Buschbaum, P. *Macromolecules* **2001**, *34*, 171.
(14) Mierzwa, M.; Floudas, G.; Wewerka, A. *Phys. Rev. E* **2001**, *64*, 31703.
(15) Mierzwa, M.; Floudas, G.; Wewerka, A *J. Non-Cryst. Solids.*, in press.
(16) Ungerank, M.; Winkler, B.; Eder, E.; Stelzer, F. *Macromol. Chem. Phys.* **1995**, *196*, 3623.
(17) Rosedale, J. H.; Bates, F. S. *Macromolecules* **1990**, *23*, 2324.
(18) Floudas, G.; Hadjichristidis, N.; Iatrou, H.; Pakula, T.; Fischer, E. W. *Macromolecules* **1994**, *27*, 7735.
(19) Han, C. D.; Kim, J. K. *Polymer* **1993**, *34*, 2533.
(20) Schrauwen, C.; Pakula, T.; Wegner, G. *Macromol. Chem.* **1992**, *193*, 11.

MA010944O